Asian Journal of Chemistry; Vol. 36, No. 6 (2024), 1286-1294

ASIAN JOURNAL OF CHEMISTRY

https://doi.org/10.14233/ajchem.2024.31384

Synergistic Effect of PVA/PVP/CuO Polymer Nanocomposites: Flexible Solid-State Asymmetric Supercapacitors

P. MUTHUMARI[1,2], A. MURUGAN[3], V. SIVA[4,5,*], A. SHAMEEM[5,6], S. ASATH BAHADUR[1,2] and S. THANGARASU[1,2,*]

[1]Department of Physics, School of Advanced Sciences, Kalasalingam Academy of Research and Education, Krishnankoil-626126, India
[2]Condensed Matter Physics Laboratory, International Research Centre, Kalasalingam Academy of Research and Education, Krishnankoil-626126, India
[3]Department of Science and Humanities, Karpagam College of Engineering, Coimbatore-641032, India
[4]Department of Physics, Karpagam Academy of Higher Education, Coimbatore-641021, India
[5]Centre for Energy and Environment, Karpagam Academy of Higher Education, Coimbatore-641021, India
[6]Department of Science and Humanities, Karpagam Academy of Higher Education, Coimbatore-641021, India

*Corresponding authors: E-mail: siva33phy@gmail.com; sthangarasu@gmail.com

Received: 12 February 2024; *Accepted*: 4 April 2024; *Published online*: 31 May 2024; AJC-21639

The electrochemical capacitors that use polymer nanocomposite electrode are the most efficient electrical energy storage devices due to their superior power density, quick charge/discharge, long cycle life and high degree of safety. The electrochemical performance of transitional metal oxide-based polymer nanocomposites electrode has been synthesized by solution casting method. The prepared polymer nanocomposites (PNCs) physical and electrochemical properties such as structural, morphology, cyclic voltammetry (CV), galvanostatic charge/discharge (GCD) and electrochemical impedance spectroscopy (EIS) were investigated. Subsequently, the solid-state asymmetric supercapacitor was assembled with (PVP/PVA/CuO X wt.%)//activated carbon in 6 M KOH electrolyte. Benefiting from the efficient pseudocapacitive properties of the flexible polymer nanocomposite positive electrode and activated carbon as a negative electrode. The PVP/PVA/5 wt.% CuO polymer nanocomposite electrode demonstrates a superior specific capacitance of 7.90 F g^{-1} at a current density of 2 A/g. The device has examined to life time application for cycling retention study and charge/discharge stability for 5 wt.% of PNCs electrode exhibited 88% capacity retention after 5000 GCD cycles at current density of 5 A g^{-1}. The assembled flexible solid-state asymmetric supercapacitor exhibits a high energy density of 6.34 Wh kg^{-1} and power density of 566.06 W kg^{-1}. These electrochemical results showed that the polymer nanocomposite exposed the strong synergistic effect between CuO nanoparticles and PVP/PVA blend polymer matrix and being facilitated by fast charge transfer, charge transfer resistance and the improved capacitance performances. Moreover, the fabricated asymmetric supercapacitors (ASCs) device also shows an excellent stability of electrochemical performance and hence finds a promising candidate for energy storage in supercapacitor as a flexible power source for wearable and portable electronics.

Keywords: PVP/PVA blend polymer, CuO nanoparticles, Polymer nanocomposite, Asymmetric supercapacitor, Energy storage.

INTRODUCTION

Renewable energy sources are indented to help with energy insufficiency and massive environmental difficulties produced with using of fossil fuels. Electrochemical energy production was one of the alternative energy sources. Recently, the effective energy management has needed the production of energy fuel which is given by an electrochemical energy storage system consisting of batteries, fuel cell and electrochemical capacitors. Electrochemical capacitors are called as supercapacitors received a lot of attention as an alternative to traditional energy storage technologies. Due to its high-power density, longer stability and superior activity than conventional energy storage devices, supercapacitors have recently emerged as promising devices [1-3].

Pseudo-capacitors have more specific capacitance and energy densities than electric double layer capacitor (EDLC). Due to its huge electrochemical capabilities, different materials such as different metal oxide nanoparticles (MnO_2, NiO, Fe_3O_4, CeO_2 and SnO_2), conducting polymers and their composition

are usually applied as pseudo-capacitor materials [4,5]. In this research, polyvinyl alcohol (PVA) has chosen much interest due to its film forming properties, biocompatibility, good chemical resistance, and it contain water degradable crystalline structure that has been easily solubilized [6,7]. Also, PVP has chosen for their mechanical efficiency and superior thermal stability, moreover, it is a good reducing agent for nanoparticle and the presence of carbonyl group tends to product metal nanoparticle within the matrix [8,9].

Polymer blending is widely known as one of the most effective method to developed novel polymeric compounds providing relevant information with different physical and chemical properties [10]. The good result of the blend polymer could be designed to get needs of requirements that could not be achieved by unique polymer. The composite made up of polymer and nanoparticle has a strong interest in developing new methods to create a new substance with desirable features that exhibit advantages in terms of different properties [11-14].

The metal oxide nanoparticle has promising results in terms of physical and chemical properties due to their higher density and limited size. Hence, the characteristics of PNC can be enhanced by adding metal oxide nanoparticle. Transition metal oxides such as ruthenium, copper, titanium and manganese oxides have shown promising potential as electrode materials for supercapacitors due to their high psudocapacitance value [15-18]. Copper oxide has inspired global interest because of its low cost, non-toxicity, a different nanoscale dimension. Among metal oxides, copper oxide has low band gap (1.2 eV) and exhibit p-type semiconductor behaviour and is considered to be one of the best supercapacitor electrode due to its superior psudocapacitance properties [19]. Hence, in this work copper oxide nanoparticle has been chosen as nanofiller to prepare the polymer nanocomposite by varied concentration. The types of PNCs attracted much attention in supercapacitor application. In this present work, a solid state flexible asymmetric supercapacitors (ASCs) using the PVA/PVP/CuO polymer nanocomposite as active material for cathode and activated carbon material as anode are developed. To the best of our knowledge to date, the present work is the first report where the fabrication of mechanically stable solid state high performance PVA/PVP/CuO asymmetric supercapacitors (ASCs) device.

EXPERIMENTAL

Polyvinyl alcohol (Mw: 90000 g/mol) and polyvinyl pyrrolidone (Mw: 1300000 g/mol) were purchased from Sigma-Aldrich, USA. Copper nitrate hexahydrate [$Cu(NO_3)_2{\cdot}6H_2O$] and ammonia solution (NH_4OH) were purchased from Merck, India and the other chemicals were used as received. The nanoparticles and polymer nanocomposites (PNCs) were prepared using ethanol and double-distilled water.

Preparation of copper oxide nanoparticles: The copper oxide nanoparticles were prepared by adopting simple co-precipitation method. In brief, 0.1 M $Cu(NO_3)_2{\cdot}6H_2O$ as precursor dissolved in 100 mL of double-distilled water and stirred for 3 h to obtain a homogenous solution. A 10 mL of NH_4OH dissolved in 100 mL of double-distilled water, thus the solution well mixed by stirring 1 h. Diluted ammonia solution was added by dropwise up to reach pH 9 and strongly stirrer in 4 h. The obtained precipitate was washed by double-distilled water and ethanol for several times to eliminate the unreacted impurities and then dried at 60 ºC for 10 h in vacuum oven. At the end, the prepared samples were calcined at 400 ºC for 4 h in muffle furnace.

Preparation of polymer nanocomposites: The polymer nanocomposites PVA/PVP/CuO (X wt.%) (X = 0.25, 0.5, 0.75, 1 and 5) were prepared by solution casting technique. In typical preparation of PVA/PVP wt.% ratio of 50:50 was taken separately under constant stirring for 3 h and then blended together to obtain homogenized viscous solution after stirring for 4 h. Now, 0.25 wt.% of CuO nanoparticles was added dropwise in a well mixed blend polymer PVA/PVP solution and stirrer for 6 h to get fine dispersion of CuO nanoparticles. The prepared mixed solution was dried at room temperature for 9 days. Similarly, the other polymer nanocomposites X wt.% (X = 0.5, 0.75, 1 and 5) were prepared by following similar process.

Characterization: Structural properties of the prepared PNCs were studied by XRD, Bruker-D8 advance ECO system by Cu$K\alpha$ radiation (λ = 1.5406 Å). Fourier transform infrared spectral studies (FTIR) of the prepared samples were carried out using Shimadzu (IR Tracer-100) spectrometer recorded in ATR mode. The morphology of the PNCs samples was analyzed by FE-SEM (Carl Zeiss Model Supra 55). Dielectric property and electrical conductivity were carried out using HIOKI 3532-50 LCR Hi-Tester in the frequency range from 42 Hz to 1 MHz.

Fabrication of asymmetric supercapacitors (ASCs) device: The ASCs supercapacitor devices were fabricated in a two-electrode configuration and studied in 6008E Electrochemical Workstation. As-prepared PVP/PVA/CuO (X wt.%) as the positive electrode and active carbon as negative electrode, both electrodes consisted the similar area of 1 cm × 2 cm. A separator composed of grade one Whattman filter paper was placed between the two electrodes and soaked in 6 M KOH electrolyte solution for 30 min. The negative electrode was prepared by 90 wt.% of activated carbon and 10 wt.% of polyvinylidene fluoride as binder and then added few drops of *N*-methyl-2-pyrrolidone to make it slurry. The slurry was glazed on nickel foil as a working in current collector. Furthermore prepared negative electrode allows to dried at 50 ºC in vacuum oven for 6 h. The positive electrode were obtained by synthesizing polymer nanocomposites (PVA/PVP/CuO X wt.%). Fig. 1 represents the model diagram of the prepared asymmetric supercapacitor (ASC) with positive and negative electrodes. The assembled ASCs device was analyzed by CHI6008E electrochemical workstation, to examine the cyclic voltammetry (CV), galvanostatic charge/discharge (GCD) and electrochemical impedance spectroscopy (EIS) studies in the alkaline electrolyte solution.

RESULTS AND DISCUSSION

XRD study: The structural properties of the prepared polymer nanocomposites were analyzed using powder XRD pattern. Fig. 2 displays the XRD patterns of the PVA/PVP/CuO polymer nanocomposites with varying weight percentages of CuO nanoparticles (X = 0.25, 0.5, 0.75, 1, and 5 wt.%). The XRD patterns of the prepared CuO nanoparticles show the

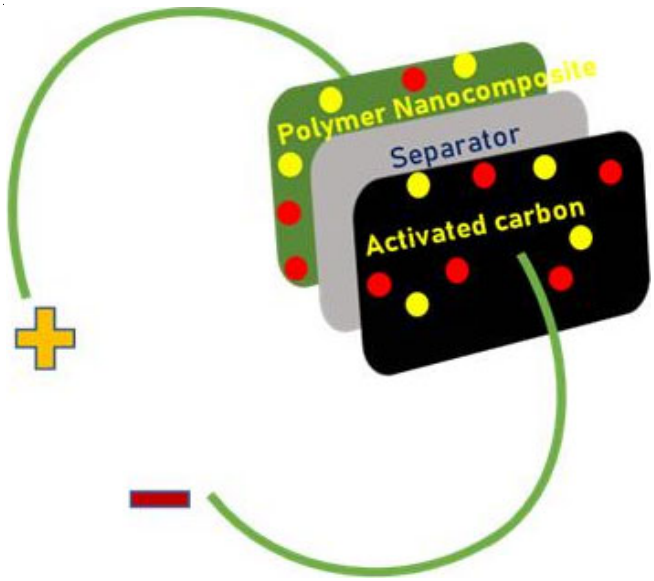

Fig. 1. Model diagram of asymmetric supercapacitor for polymer nanocomposite

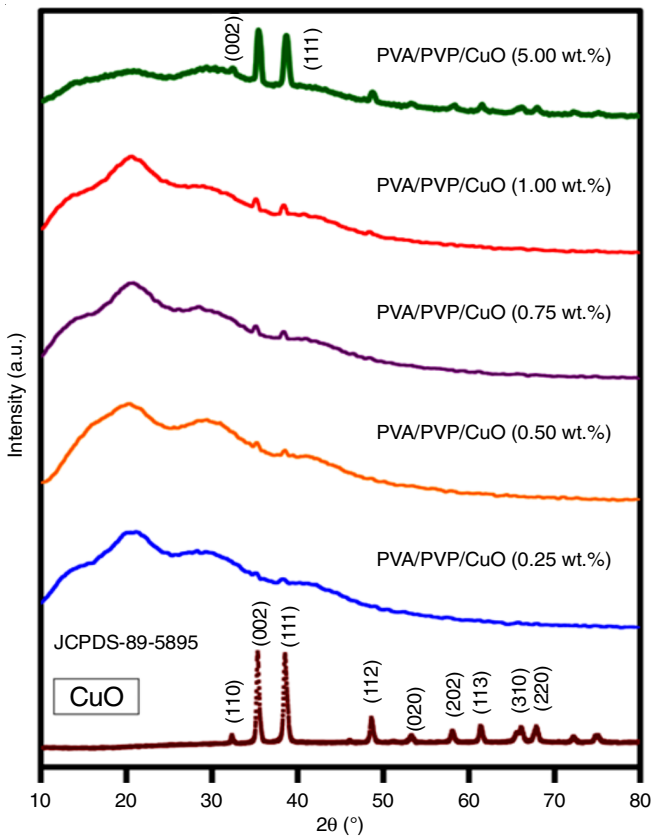

Fig. 2. XRD graph for PVA/PVP/CuO X wt.% (X = 0.25, 0.5, 0.75, 1 and 5)

diffraction peaks at 2θ about 32.49º, 35.57º, 38.61º, 48.78º, 53.38º, 58.36º, 61.48º, 66.30º, 68.12º, 72.46º which is confirmed by purity of the prepared nanoparticles. These diffraction peaks were well-matched with JCPDS No. 89-5895. The addition of CuO nanoparticles to the blend polymer resulted in a decrease in the amorphous form of the polymer as the weight percentage of nanoparticles increased. The wide peak is detected in the low diffraction angle for all weight percentages of polymer nanocomposites, indicating the amorphous nature of the blended polymer. Furthermore, the XRD pattern of PVP/PVA/CuO (X wt.%) polymer nanocomposites exhibits the prominent peaks of higher intensity as increasing wt.% of CuO nanoparticles, which suggests that the combination of polymer nanocomposite components is highly effective. The crystallite size was calculated using Scherrer's formula based on the most intense peak in CuO NPs and PVA/PVP/CuO (X wt.%) polymer nanocomposites.

$$D = \frac{K\lambda}{\beta\cos\theta}$$

where D is crystallite size (nm), K is shape factor, λ is wavelength of Cu*K*α (λ = 1.54056 Å), β is full width at half of maximum in diffraction (*hkl*) peak and θ is diffraction angle. The calculated crystallite size was approximately 45, 50, 51 and 49 nm for CuO NPs, 0.5 wt.%, 0.5 wt.%, 0.75 wt.% and 5 wt.% of polymer nanocomposites, respectively.

Morphology studies

SEM studies: The irregular shaped particles and particle agglomerates are visible on the surface of a granular structure. The pure form of CuO has a granular texture characterized by compact bonded particles. The energy dispersive spectra of the sample were used to determine the purity and chemical composition of the synthesized material. Only elemental copper (Cu) and oxygen (O), no other elemental impurities were found in the EDS spectrum (Fig. 3).

FE-SEM analysis: Fig. 4 reveals the FESEM images of PVA/PVP/CuO (X wt.%) (X = 0.25, 0.5, 0.75, 1.0, 5.0). The FESEM micrographs of PVA/PVP/CuO clearly showed that uniform morphology and fine dispersion of copper oxide into the PVA/PVP blend matrix. It could be observed that the surface morphology of 0.25 wt.% of CuO is obviously different from that of 5 wt.% of CuO in polymer matrix. Furthermore, the rough and porous structure on the surface of polymer becomes more evident and consistent as the CuO content increases, in contrast to the 0.25 wt.% CuO in PVA/PVP. As shown in Fig. 4, the concentration of CuO nanoparticles in the PVA/PVP matrix, leads to the formation of large agglomerates.

Electrochemical studies

Cyclic voltammetry: In order to learn more about the possibilities of various PVA/PVP/CuO (X wt.%) PNCs as cathode electrode materials for energy storage in supercapacitors, the electrochemical performance of different wt.% of ASCs device was examined by cyclic voltammetry, galvanostatic charge-discharge and electrochemical impedance spectroscopy in alkaline electrolyte. The PVA/PVP/CuO (X wt.%)//activated carbon ASCs device was fabricated using two electrode system by PVA/PVP/CuO (X wt.%) as positive electrode and activated carbon as a negative electrode.

Fig. 5 displays the CV profiles of ASCs device and potential window of 0 to 1.9 V with different scan rate of 5 to 150 mV/s. The CV profiles of ASCs device exhibit the pseudocapacitance behaviour (Faradic redox reaction). The redox reaction of Cu^{+}/Cu^{2+} has a synergistic effect of blended PVA/PVP polymer, because it is an electrochemically active substance [20]. The

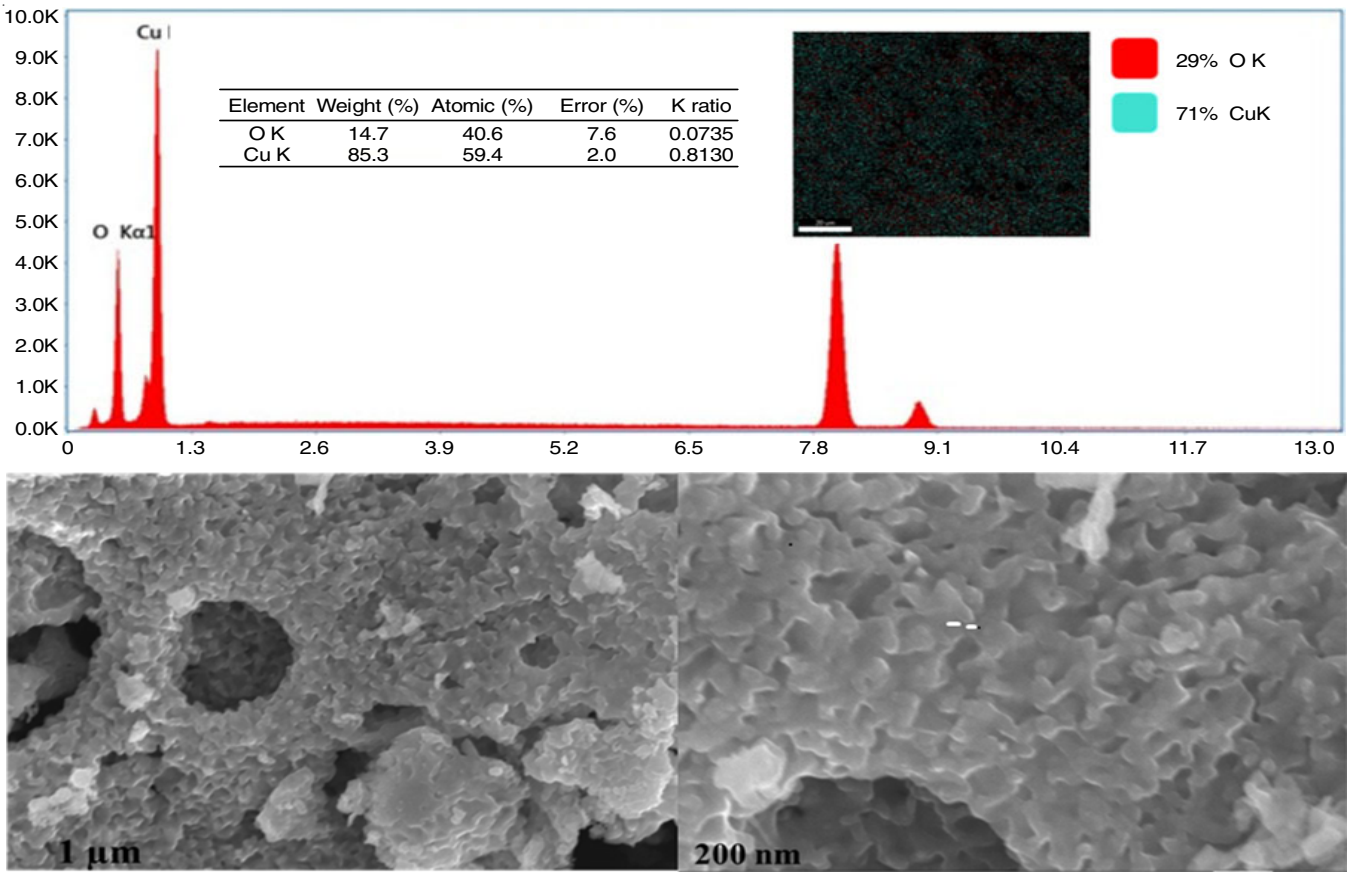

Fig. 3. SEM and EDAX spectrum of CuO

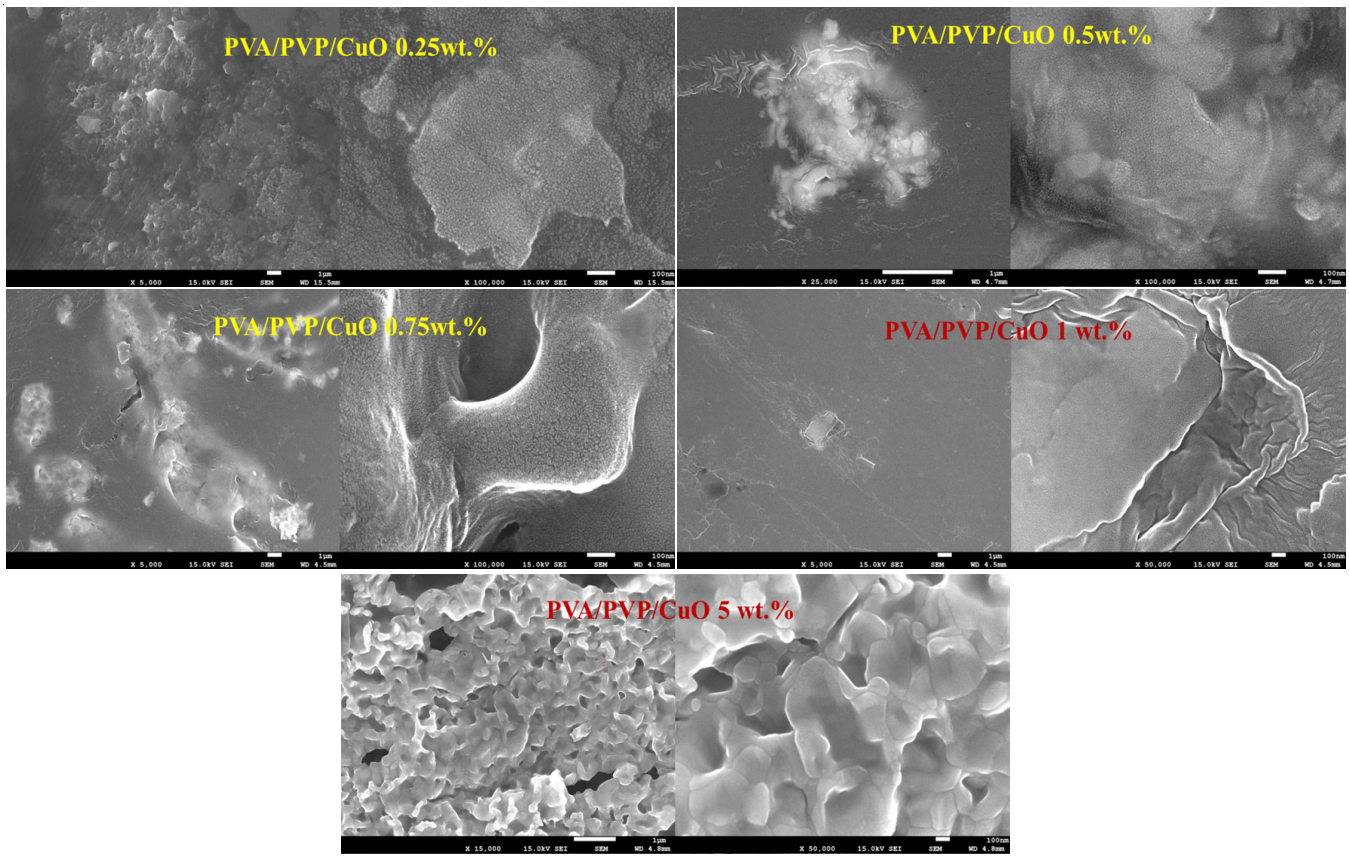

Fig. 4. FESEM images of PVA/PVP/CuO X wt.% (X = 0.25, 0.5, 0.75, 1 and 5)

wt.% of CuO nanoparticles increased with the current density of CV profiles, which is indicated by the well-redox reaction of the ASCs device and the area of the CV curve increased with respect to increasing wt.% of CuO NPs, which is shown in the energy storage of the electrode. The specific capacitance of assembled ASCs device was calculated by following equations [21]:

$$C_{sp}(\text{Gravimetric}) = \frac{\int IdV}{m \times v \times \Delta V} F/g$$

where C_{sp} = specific capacitance (F g^{-1}), $\int IdV$ = area of CV profiles, m = mass of ASCs device (g), v = scan rate and ΔV = potential window (V). The calculated C_{sp} are listed in Table-1.

The specific capacitance of the ASCs device (0.25 wt.% to 5 wt.%) attain from the CV measurements are 9.2 F/g, 11.9 F/g, 13.9 F/g and 21.6 F/g for PVA/PVP/CuO (X wt.%) at a scan rate of 5 mV/s. The higher specific capacitance 40.2 F/g is attained for PVA/PVP/CuO 5 wt.% as shown in Table-1. From Fig. 5e, the redox processes at the electrode and electrolyte interface were initiated by the higher concentration of CuO and these redox peaks were much visible at 5 wt.% of CuO. Particularly, the PVA/PVP/CuO 5 wt.% sample gained larger area which then yielded higher specific capacitance amounting to 40.2 F/g. The redox reaction of the PVA/PVP/CuO electrode might be represented by the following mechanism:

$$2CuO + H_2O + 2e^- \rightleftharpoons Cu_2O + 2OH^-$$

Furthermore, as the scan rate increased, the specific capacitance decreased, may be due to the reduction of active participation of ions within the active material at higher scan rates. An electrolyte also contributes to improve the specific capacitance. The comparison CV graphs for PVA/PVP/CuO (X wt.%) at 5 mV/s scan rate and the comparison plot of PVA/PVP/CuO (X wt.%) for different scan rate *vs.* specific capacitance are shown in Figs. 6 and 7, respectively. These plots are additional reference to confirm the higher specific capacitance obtained for PVA/PVP/CuO 5 wt.%.

Galvanostatic charge and discharge: The charge-discharge of prepared ASCs device were examined at different current densities and are shown in Fig. 8a-f. The GCD profiles

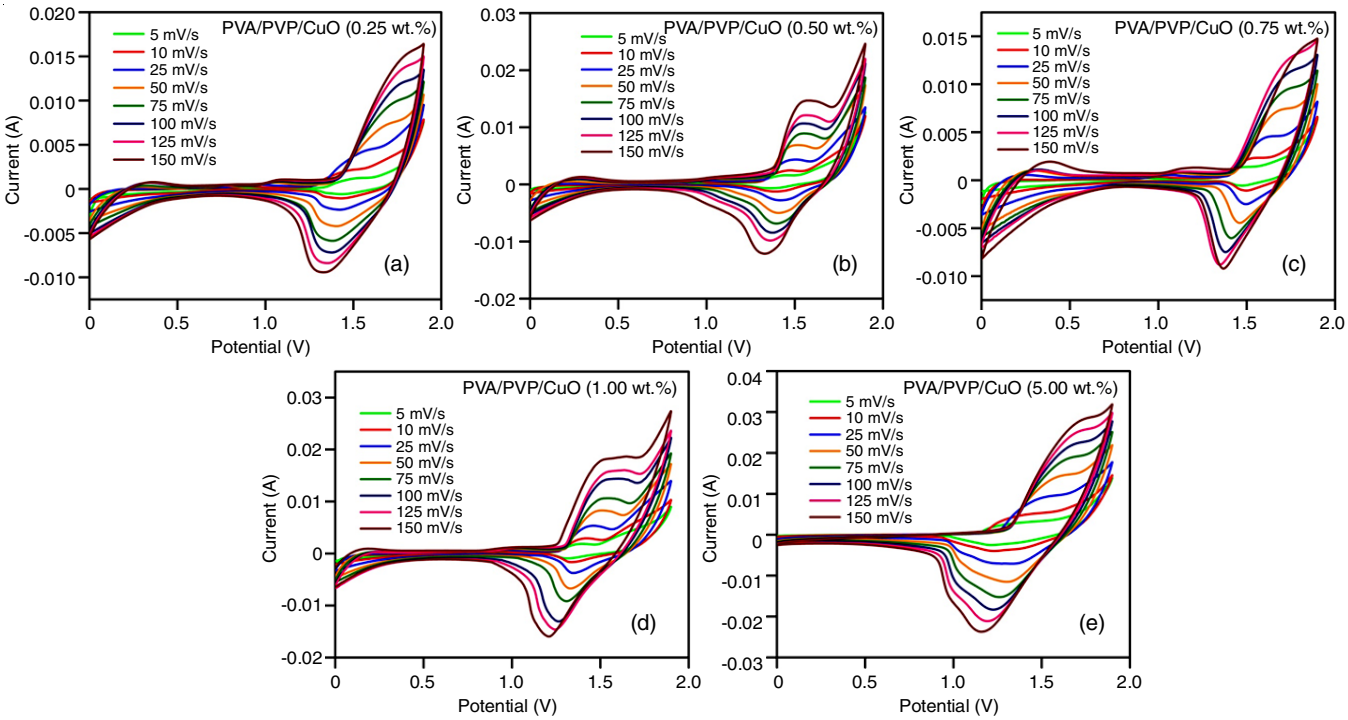

Fig. 5. Cyclovoltagrams of PVA/PVP/CuO X wt.% (X = 0.25, 0.5, 0.75, 1 and 5) at different concentration

TABLE-1
SPECIFIC CAPACITANCE VALUES FOR PVA/PVP/CuO X wt.%

Scan rate (mV/s)	Specific capacitance PVA/PVP/CuO X wt.% from CV									
	0.25		0.50		0.75		1.00		5.00	
	F/g	mF/m^2	F/g	mF/m^2	F/g	mF/m^2	F/g	mF/m^2	F/g	mF/m^2
5	9.2	55.3	11.9	65.5	13.9	76.8	21.6	97.4	40.2	160.9
10	8.0	48.2	9.59	52.7	11.0	60.9	16.5	74.6	34.2	136.6
25	6.7	40.3	7.11	39.1	8.0	44.0	11.3	51.06	22.4	89.6
50	4.5	27.5	5.20	28.6	6.2	34.5	8.1	36.63	15.4	61.7
75	3.9	23.5	4.18	23.0	5.02	27.5	6.78	30.53	12.6	50.5
100	3.4	20.6	3.62	19.9	4.49	24.7	5.08	24.49	10.8	43.6
125	3.1	18.6	3.22	17.7	4.00	22.1	5.03	22.90	9.7	38.9
150	2.8	16.9	2.74	15.1	3.92	22.0	4.71	22.06	8.9	35.7

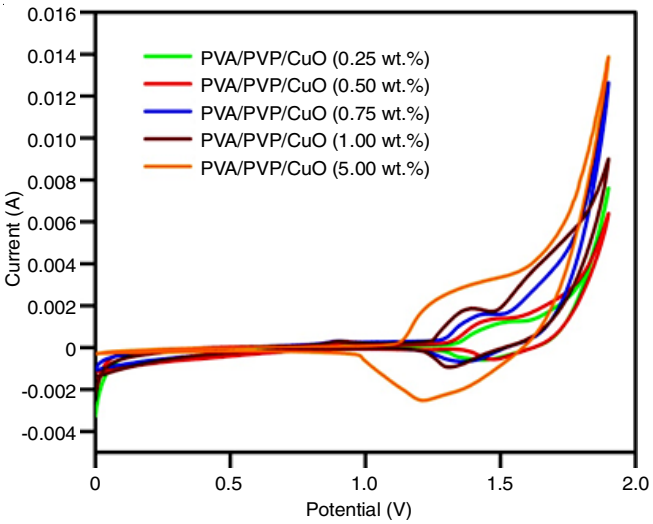

Fig. 6. Comparative CV graphs for PVA/PVP/CuO X wt.% (X = 0.25, 0.5, 0.75, 1 and 5) at 5 mV/s scan rate

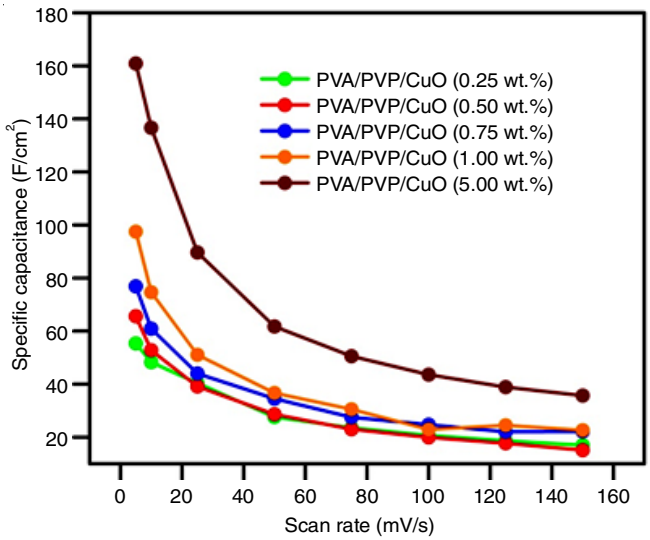

Fig. 7. Comparative plot of PVA/PVP/CuO X wt.% (X = 0.25, 0.5, 0.75, 1 and 5) for different scan rate *vs.* specific capacitance

displayed a non-triangular form indicating its pseudocapacitive nature resulting from the Faradic redox reactions. The gravimetric and areal specific capacitance can be determined using GCD discharge time by the following equations [22]:

$$C_{sp}(F\,g^{-1}) = \frac{I \times dt}{m \times \Delta V}$$

$$C_{sp}(F\,cm^{-1}) = \frac{I \times dt}{A \times \Delta V}$$

where C_{sp} = specific capacitance, I = applied current density in A, Δt = discharging time in s, m = mass of polymer nanocomposites in g, ΔV = potential window (V), A = surface area of polymer nanocomposite (cm).

The specific capacitance calculated from the GCD characteristics for the PNCs (0.25 wt.% to 5 wt.%) are 2.82 F/g, 3.67 F/g, 4.01 F/g, 7.72 F/g and 7.90 F/g at 1 A/g (Table-2). Areal capacitance also calculated and the values are 16.95 mF/cm^2, 20.20 mF/cm^2, 22.06 mF/cm^2, 34.74 mF/cm^2 and 67.18 mF/cm^2. According to their structure and morphology, which help in the good interaction and provide synergism among the polymer nanocomposite, the PVA/PVP/CuO 5 wt.% PNC electrode exhibits a higher specific capacitance as shown in Table-2. Because of the electrolyte's ion diffusion, the internal resistance of the discharge curves during fast charging and discharging exhibits low internal resistance [23].

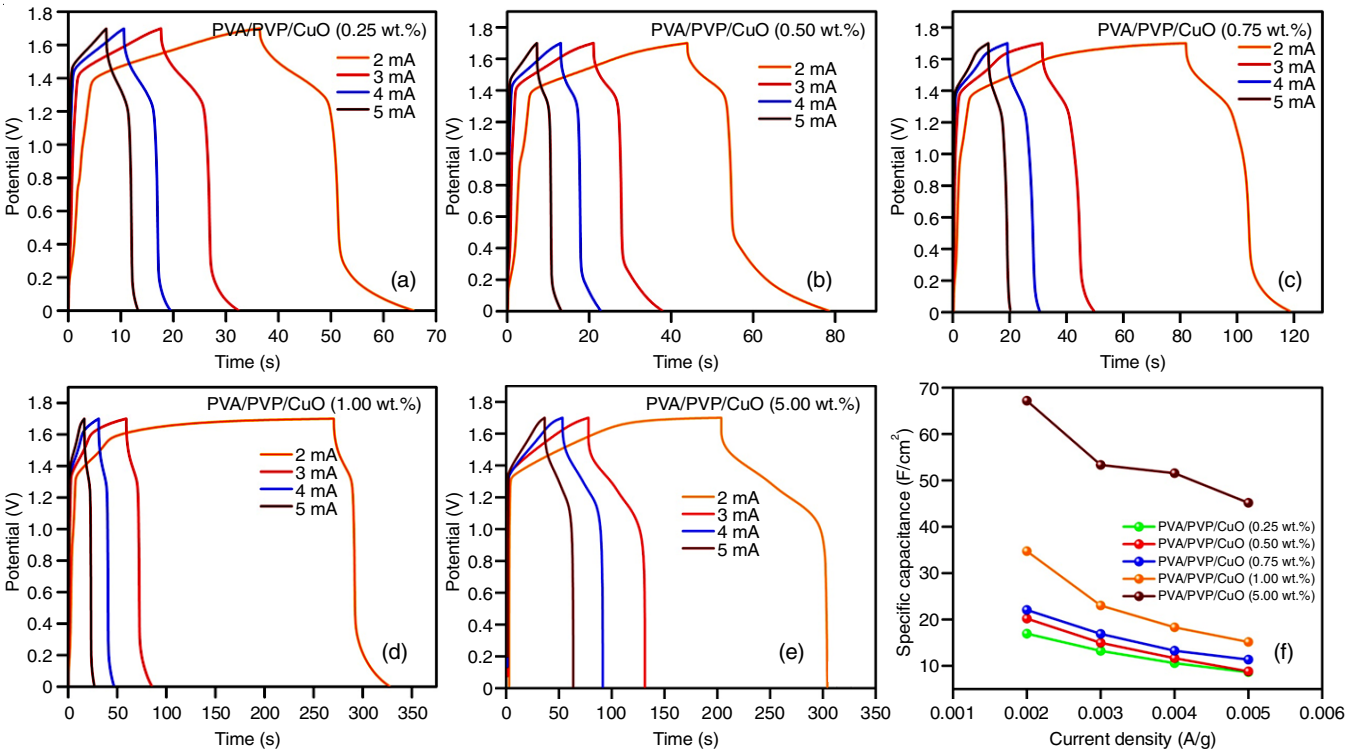

Fig. 8. GCD graphs for PVA/PVP/CuO X wt.% (X = 0.25, 0.5, 0.75, 1 and 5) at 1.7 V

TABLE-2
SPECIFIC CAPACITANCE DATA OF PVA/PVP/CuO X wt.% FROM GCD TECHNIQUE

Current density (A/g)	Specific capacitance PVA/PVP/CuO X wt.% from GCD									
	0.25		0.50		0.75		1.00		5.00	
	F/g	mF/m^2	F/g	mF/m^2	F/g	mF/m^2	F/g	mF/m^2	F/g	mF/m^2
2	2.82	16.95	3.67	20.20	4.01	22.06	7.72	34.74	7.90	67.18
3	2.20	13.23	2.72	14.97	3.07	16.88	5.11	23.02	6.27	53.32
4	1.76	10.58	2.11	11.65	2.41	13.28	4.07	18.31	6.06	51.54
5	1.44	8.64	1.60	8.82	2.06	11.35	3.36	15.16	5.31	45.16

For an electrochemical device, a cycling stability is one of the important for practical application. The cycling performance of PVA/PVP/CuO (X wt.%) device for 5000 cycles in 3 M KOH solution at a current density of 5 mA in potential window of 0 to 1.7 V was carried out to test the stability of asymmetric supercapacitor device as shown in Fig. 9. The ratio of discharge capacitance to the charge capacitance can be used to calculate the columbic efficiency. The columbic efficiency was calculated by the following equation [24]:

$$\eta = \frac{t_d}{t_c} \times 100\%$$

where t_d = total amount of discharge and t_c = total amount of charge.

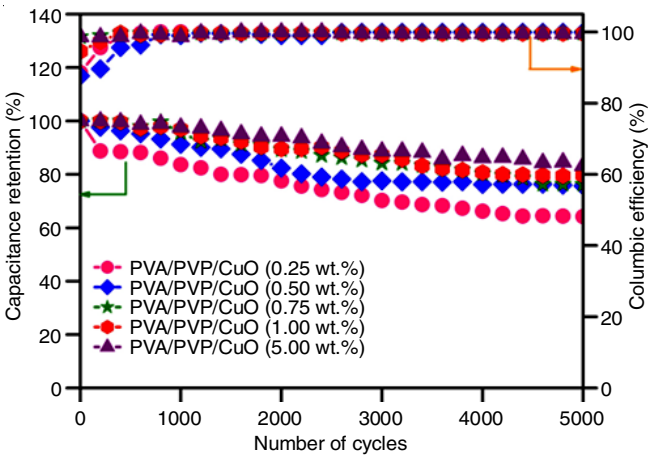

Fig. 9. GCD graphs for capacitance retention and columbic efficiency of PVA/PVP/CuO 5 wt% at 1.7 V

For the asymmetric supercapacitor device PVA/PVP/CuO (X wt.%) (X = 0.25, 0.5, 0.75, 1.0, 5.0 wt.%) shows the capacitance decreases gradually with the cycle number increase and shows 64.23%, 75.73%, 76.25%, 79.63%, 83.23% of capacitance retention, respectively after 5000 cycles has remarkable cyclic stability. The Ragone plot of PVA/PVP/CuO (X wt.%) representing the energy density and power density is depicted in Fig. 10. The energy density and power density were calculated by following equation and the values are listed in Table-3.

$$E\ (Wh\ K\ g^{-1}) = \frac{C_{sp} \times \Delta V^2}{7.2}$$

$$P\ (W\ K\ g^{-1}) = \frac{E \times 3600}{\Delta t}$$

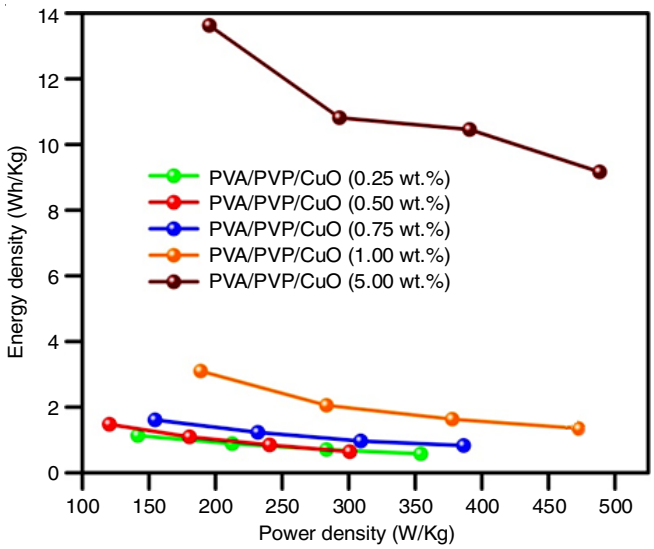

Fig. 10. Comparison of specific capacitance of PVA/PVP/CuO X wt.% (X = 0.25, 0.5, 0.75, 1 and 5) *vs.* current density

TABLE-3
ENERGY DENSITY *vs.* POWER DENSITY

PVA/PVP/CuO X (wt.%)	Energy density (Wh kg^{-1})	Power density (W kg^{-1})
0.25	1.13	354.16
0.50	1.47	300.80
0.75	1.61	386.36
1.00	3.09	472.22
5.00	6.34	566.06

Electrochemical impedance spectroscopy (EIS): Electrochemical impedance spectroscopy was used to examine the electrochemical behaviour of ASCs device. The Nyquist plot of the ASCs device for before GCD and after GCD 5000 cycle was analyzed in the frequency of 1 Hz to 100 kHz and shown in Fig. 11a-e. At high frequencies region a small semi-circle is appeared at the lower frequencies side. Usually, the charge transfer resistance (R_{ct}) defines the semicircle diameter and the low frequency straight line shows that the prepared materials are pseudocapacitive. A almost straight line in the low frequency reflects the perfect capacitive behaviour and the low equivalent series resistance reveals the low internal resistance of the device [25]. According to the equivalent circuit involving the solution resistance (R_s) and the charge transfer resistance (R_{ct}) were calculated (Table-4). Due to its low interfacial charge resistance and good conductivity, these results indicated that the PVA/PVP/CuO PNCs electrode materials are suitable for the energy storage in supercapacitor.

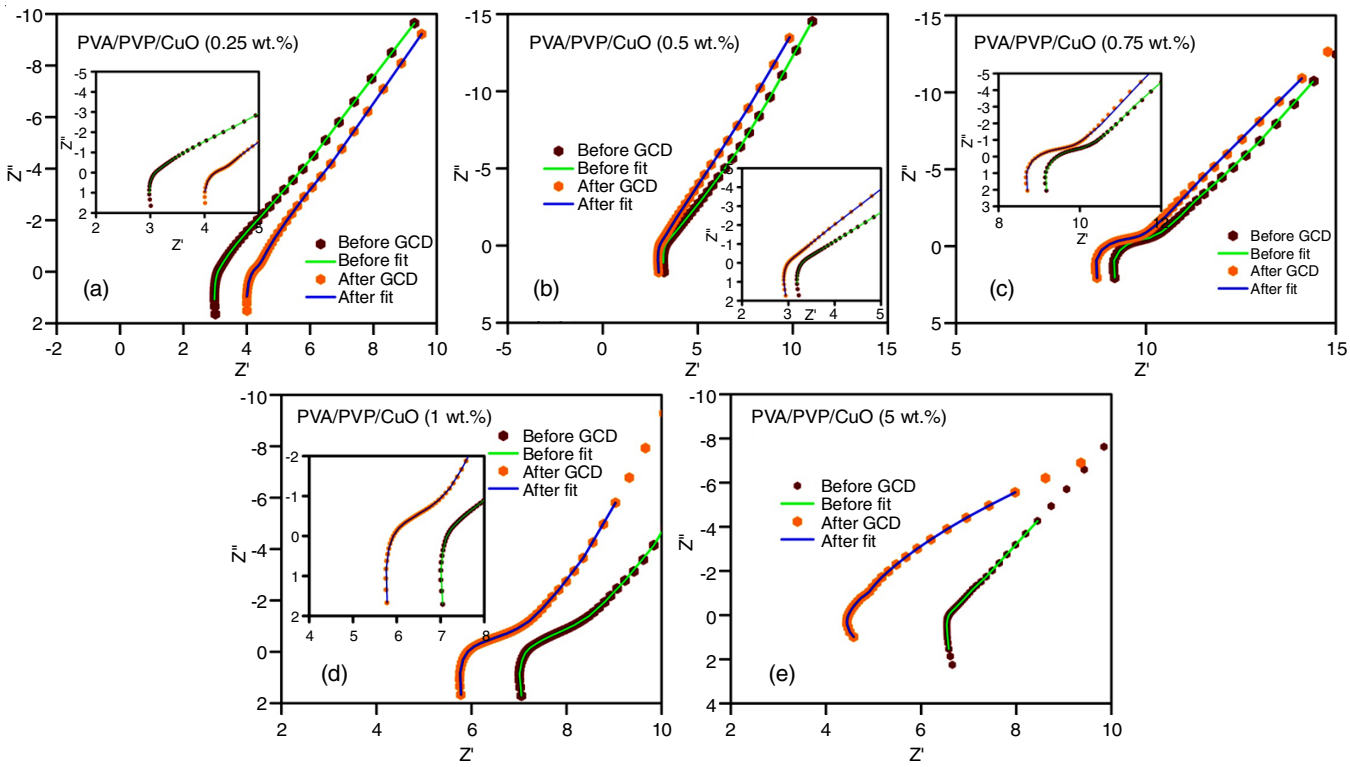

Fig. 11. EIS plots for PVA/PVP/CuO X wt.% (X = 0.25, 0.5, 0.75, 1 and 5)

TABLE-4
R_s AND R_{ct} VALUES OF PVA/PVP/CuO X wt.%

	CuO 0.25 wt%		CuO 0.50 wt%		CuO 0.75 wt%		CuO 1.00 wt%		CuO 5.00 wt%	
	Before GCD	After GCD	Before GCD	After GCD	Before GCD	After GCD	Before GCD	After GCD	Before GCD	After GCD
R_s	3.00	4.03	3.21	2.89	9.17	8.70	7.07	5.78	6.53	4.44
R_{ct}	1.24	0.64	1.64	1.39	0.95	1.04	0.70	0.76	0.42	0.83

Conclusion

The PVP/PVA/CuO (X wt.%) polymer nanocomposites were prepared by simple solution casting method. The structural properties and morphology were studied by XRD and FESEM techniques. The FESEM images of PVA/PVP/CuO showed a uniform distribution of copper oxide nanostructures into the PVA/PVP matrix. The fabricated devices PVA/PVP/CuO were characterized for electrochemical properties in 6 M KOH electrolyte. The PVA/PVP/5 wt.% CuO polymer nanocomposite based asymmetric supercapacitors (ASCs) device excelled a higher specific capacitance of 7.90 F/g and 67.18 mF/cm^2 at current density of 2 A/g which is very high capacitance than other wt.% CuO and retained 88% of capacitance at 5000 cycles with a coulombic efficiency of 96%. The obtained energy density and power density were 6.34 Wh/Kg and 566.06 W/Kg, respectively. The PVA/PVP/CuO polymer nanocomposite must be studied extremely for achieving high performance electrode.

CONFLICT OF INTEREST

The authors declare that there is no conflict of interests regarding the publication of this article.

REFERENCES

1. C. Largeot, C. Portet, J. Chmiola, P.L. Taberna, Y. Gogotsi and P. Simon, *J. Am. Chem. Soc.*, **130**, 2730 (2008); https://doi.org/10.1021/ja7106178
2. S. Chen, J. Zhu, X. Wu, Q. Han and X. Wang, *ACS Nano*, **4**, 2822 (2010); https://doi.org/10.1021/nn901311t
3. M.D. Stoller, S. Park, Y. Zhu, J. An and R.S. Ruoff, *Nano Lett.*, **8**, 3498 (2008); https://doi.org/10.1021/nl802558y
4. R. Etefagh, S. Rozati, E. Azhir, N. Shahtahmasebi and A. Hosseini, *Sci. Iran.*, **24**, 1717 (2017); https://doi.org/10.24200/SCI.2017.4147
5. C. DeMerlis and D. Schoneker, *Food Chem. Toxicol.*, **41**, 319 (2003); https://doi.org/10.1016/S0278-6915(02)00258-2
6. J. Arjomandi, J.Y. Lee, R. Movafagh, H. Moghanni-Bavil-Olyaei and M.H. Parvin, *J. Electroanal. Chem.*, **810**, 100 (2018); https://doi.org/10.1016/j.jelechem.2017.12.086
7. M. Yassine and D. Fabris, *Energies*, **10**, 1340 (2017); https://doi.org/10.3390/en10091340
8. A.T. Florence, *Int. J. Pharm.*, **551**, 1 (2018); https://doi.org/10.1016/j.ijpharm.2018.08.023
9. E.M. Abdelrazek, A.M. Abdelghany, S.I. Badr and M.A. Morsi, *J. Mater. Res. Technol.*, **7**, 419 (2018); https://doi.org/10.1016/j.jmrt.2017.06.009
10. A.M. Abdelghany, A.A. Menazea and A.M. Ismail, *J. Mol. Struct.*, **1197**, 603 (2019); https://doi.org/10.1016/j.molstruc.2019.07.089

11. M.A. Morsi, A. Rajeh and A.A. Menazea, *J. Mater. Sci. Mater. Electron.*, **30**, 2693 (2019); https://doi.org/10.1007/s10854-018-0545-4
12. I.S. Elashmawi and A.A. Menazea, *J. Mater. Res. Technol.*, **8**, 1944 (2019); https://doi.org/10.1016/j.jmrt.2019.01.011
13. A.A. Menazea, S.A. Abdelbadie and M.K. Ahmed, *Appl. Surf. Sci.*, **508**, 145299 (2020); https://doi.org/10.1016/j.apsusc.2020.145299
14. A.A. Menazea, *J. Mol. Struct.*, **1207**, 127807 (2020); https://doi.org/10.1016/j.molstruc.2020.127807
15. Y.T. Kim, K. Tadai and T. Mitani, *J. Mater. Chem.*, **15**, 4914 (2005); https://doi.org/10.1039/b511869g
16. J. Shaikh, R. Pawar, N. Tarwal, D. Patil and P. Patil, *J. Alloys Compd.*, **509**, 7168 (2011); https://doi.org/10.1016/j.jallcom.2011.04.040
17. A.E. Fischer, K.A. Pettigrew, D.R. Rolison, R.M. Stroud and J.W. Long, *Nano Lett.*, **7**, 281 (2007); https://doi.org/10.1021/nl062263i
18. S.K. Shinde, D.P. Dubal, G.S. Ghodake and V.J. Fulari, *RSC Advances*, **5**, 4443 (2015); https://doi.org/10.1039/C4RA11164H
19. M. Shahmiri, N.A. Ibrahim, W.M.Z.W. Yunus, K. Shameli, N. Zainuddin and H. Jahangirian, *Adv. Sci. Eng. Med.*, **5**, 193 (2013); https://doi.org/10.1166/asem.2013.1227
20. V. Bhavsar and D. Tripathi, *J. Polym. Eng.*, **38**, 419 (2018); https://doi.org/10.1515/polyeng-2017-0184
21. K.J. Arun, A.K. Batra, A. Krishna, K. Bhat, M.D. Aggarwal and P.J. Joseph Francis, *Am. J. Mater. Sci.*, **5**, 36 (2015).
22. E.M. Abdelrazek and H.M. Ragab, *Indian J. Phys.*, **89**, 577 (2015); https://doi.org/10.1007/s12648-014-0621-4
23. N. Ghosh, S. Sen, G. Biswas, L.R. Singh, D. Chakdar and P.K. Haldar, *Int. J. Environ. Anal. Chem.*, (2022); https://doi.org/10.1080/03067319.2022.2060088
24. V.D. Mote, Y. Purushotham and B.N. Dole, *Mater. Des.*, **96**, 99 (2016); https://doi.org/10.1016/j.matdes.2016.02.016
25. M.P. Ahmad, A. Venkateswara Rao, K.S. Babu and G.N. Rao, *Mater. Chem. Phys.*, **224**, 79 (2019); https://doi.org/10.1016/j.matchemphys.2018.12.002